**Supporting Information.** Liao, J., G. Barabás, and D. Bearup. 2021. Competition-colonization dynamics and multimodality in diversity-disturbance relationships. Ecology.

## Appendix S1

### Section S1. Classic C-C model is a special case of the generalized C-C model

The classic competition-colonization (C-C) model developed by Tilman (1994) is a special case of our modelling framework. Tilman's model can be written as

$$\frac{dp_i}{dt} = c_i p_i\left(1 - \sum_{j=1}^{i} p_j\right) - e_i p_i - \sum_{j=1}^{i-1} c_j p_j p_i, \qquad \text{Equation S1}$$

with a competitive hierarchy by ranking the species from the best competitor (species 1) to the poorest (species $n$). In our model, we have $H_{ij}$=1 and $H_{ji}$=0 if $i<j$ ($i$ and $j$ are species identity, i.e. 1, 2, 3...$n$), while $H_{ij}$=0 and $H_{ji}$=1 if $i>j$, according to the strict competitive hierarchy (note $H_{ij}+H_{ji}$=1). As such, we have

$$\begin{aligned}\frac{dp_i}{dt} &= c_i p_i\left(1 - \sum_{j=1}^{n} p_j\right) - e_i p_i + \sum_{j=1}^{n}\left(c_i p_i H_{ij} p_j - c_j p_j H_{ji} p_i\right) \qquad \text{Equation S2}\\ &= c_i p_i - c_i p_i\left(\sum_{j=1}^{i} p_j + \sum_{j=i+1}^{n} p_j\right) - e_i p_i + \sum_{j=1}^{n}\left(c_i p_i H_{ij} p_j - c_j p_j H_{ji} p_i\right),\end{aligned}$$

in which $c_i p_i H_{ij} p_j$=0 when $i>j$ (as $H_{ij}$=0 and $H_{ji}$=1), and $c_j p_j H_{ji} p_i = 0$ if $i<j$ (as $H_{ji}$=0 and $H_{ij}$=1). Here $H_{ii}$=0 for all diagonal elements in the zero-sum tournament matrix $H$. Thus we obtain

$$\begin{cases}\sum_{j=1}^{n} c_i p_i H_{ij} p_j = \sum_{j=i+1, j>i}^{n} c_i p_i p_j \\ \sum_{j=1}^{n} c_j p_j H_{ji} p_i = \sum_{j=1, j<i}^{i-1} c_j p_j p_i\end{cases}. \qquad \text{Equation S3}$$

Integrating these expressions into our modelling framework above (Appendix S1: Equation S2), we have

$$\frac{dp_i}{dt} = c_i p_i - c_i p_i\left(\sum_{j=1}^{i} p_j + \sum_{j=i+1}^{n} p_j\right) - e_i p_i + c_i p_i \sum_{j=i+1}^{n} p_j - \sum_{j=1}^{i-1} c_j p_j p_i$$

$$\frac{dp_i}{dt} = c_i p_i - c_i p_i \sum_{j=1}^{i} p_j - e_i p_i - \sum_{j=1}^{i-1} c_j p_j p_i$$

$$\frac{dp_i}{dt} = c_i p_i\left(1 - \sum_{j=1}^{i} p_j\right) - e_i p_i - \sum_{j=1}^{i-1} c_j p_j p_i, \qquad \text{Equation S4}$$

which is the same as Tilman's model as shown in Appendix S1: Equation S1.

**Literature cited**

Tilman, D. 1994. Competition and biodiversity in spatially structured habitats. Ecology 75:2–16.

**Supporting Information.** Liao, J., G. Barabás, and D. Bearup. 2021. Competition-colonization dynamics and multimodality in diversity-disturbance relationships. Ecology.

## Appendix S2

### Section S1. General properties of the disturbed model

Disturbance is introduced in our model via the forcing function $f(t,D,T)$:

$$\frac{dp_i}{dt} = c_i p_i\left(1 - \sum_{j=1}^{n} p_j\right) - e_i p_i + \sum_{j=1}^{n}\left(c_i p_i H_{ij} p_j - c_j p_j H_{ji} p_i\right) + p_i f(t,D,T). \quad \text{Equation S1}$$

The forcing function removes a fraction $D$ of each species within each period $T$, though the function itself need not be periodic. We rearrange the equation:

$$\frac{dp_i}{dt} = p_i\left[\underbrace{c_i - e_i + f(t,D,T)}_{b_i} + \sum_{j=1}^{n}\underbrace{\left(c_i H_{ij} - c_j H_{ji} - c_i\right)}_{A_{ij}} p_j\right], \quad \text{Equation S2}$$

where the $b_i$ are effective intrinsic growth rates, $A_{ij}$ are effective interaction coefficients, and the bracketed term above is the *per-capita* growth rate $r_i = \frac{1}{p_i}\frac{dp_i}{dt}$ of species *i*. In this notation, the per capita rates are manifestly linear in the $p_i$, and have the Lotka-Volterra form

$$r_i = b_i + \sum_{j=1}^{n} A_{ij} p_j. \quad \text{Equation S3}$$

This linearity means that one can take the time-average of these growth rates directly:

$$\bar{r}_i = \bar{b}_i + \sum_{j=1}^{n} A_{ij}\bar{p}_j, \quad \text{Equation S4}$$

where the over-bar denotes time averaging. If we simply replace the fluctuating model with the one where parameters are set to their time-averages obtained from the fluctuating model, the long-term outcomes will not change.

In our case, $p_i$ drops to $(1-D)p_i$ during every period $T$. Thus we replace the mortality rate $e_i$ with $e_i - log(1-D)/T$, which gives the same long-term average result as the periodically-disturbed model. To explain this, we simply calculate how

much mortality a rate of $log(1-D)/T$ causes within one period $T$. Integrating $dp_i/dt = [log(1-D)/T]p_i$ over time, we get $p_i(t) = exp[log(1-D)^{t/T}] \cdot p_i(0)$, or equivalently, $p_i(t) = p_i(0) \cdot (1-D)^{t/T}$, which gives $p_i(T) = (1-D)p_i(0)$ for $t = T$. We therefore have

$\bar{b}_i = c_i - e_i + log(1-D)/T.$ Equation S5

Writing this back into Appendix S2: Equation S4, we have

$\bar{r}_i = (c_i - e_i + log(1-D)/T) + \sum_{j=1}^{n} A_{ij}\bar{p}_j.$ Equation S6

Due to the time averaging, the steady-state is now characterized by all average *per-capita* growth rates being equal to zero: $\bar{r}_i = 0$. At this steady state, Appendix S2: Equation S6 reads

$0 = (c_i - e_i + log(1-D)/T) + \sum_{j=1}^{n} A_{ij}\bar{p}_j^*,$ Equation S7

where $\bar{p}_i^*$ are the average site occupancies of species *i* at steady state. We can express these site occupancies explicitly, by inverting the matrix $A$:

$\bar{p}_i^* = -\sum_{j=1}^{n} (A^{-1})_{ij}[c_j - e_j + log(1-D)/T],$ Equation S8

where $(A^{-1})_{ij}$ is the $(i,j)$th entry of $A$'s inverse. Appendix S2: Equation S8 gives the average stationary site occupancies in response to a disturbance of period $T$ and extent $D$.

Appendix S2: Equation S8 depends on both the extent and periodicity of the disturbance. Fortunately, the effects of varying *T* can be fully understood, because a disturbance regime with periodicity *T* and extent *D* is exactly equivalent to another one with period *T'* = 1 and extent

$D' = 1 - (1-D)^{1/T}.$ Equation S9

Indeed, considering that the average effect of disturbance is a $-log(1-D)/T$

contribution to mortality (Appendix S2: Equation S5) and therefore requiring $log(1 - D') = log(1 - D)/T$ to hold, we immediately arrive at Appendix S2: Equation S9 after solving for *D'*. For example, Appendix S2: Fig. S1 below demonstrates this for the diversity-disturbance curves of two 4-species communities: one with *T* and *D* and the other with *T'* = 1 and *D'*. As shown, the two curves are identical, as they should be. In conclusion, any change in *T* can be understood as a change to *D* instead, via Appendix S2: Equation S9, keeping *T* equal to 1.

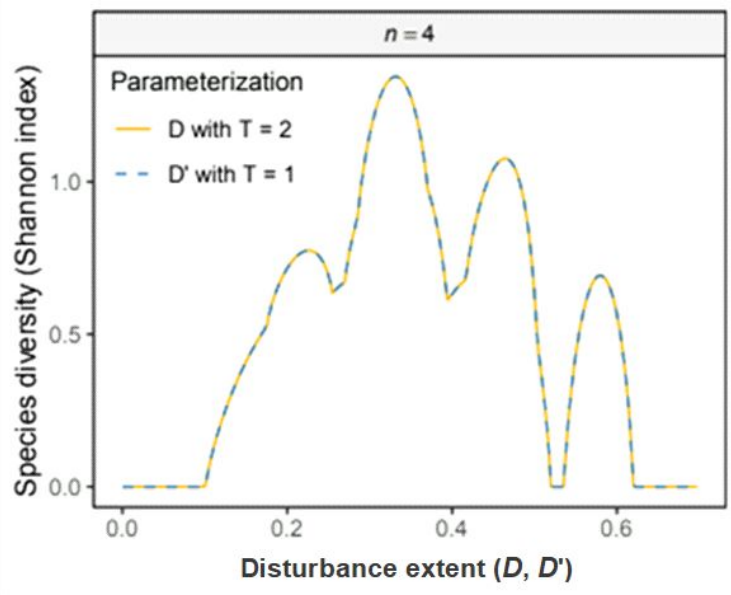


**Figure S1.** Effect of varying disturbance periodicity (*T*=1 and 2) on DDRs at equilibrium in a 4-species system with a strict competitive hierarchy *H*. Note both the dashed red line (*T* = 2) and the solid blue one (*T* = 1) fully overlap. Parameters: species mortality rates are all equal to $e_i$ = 0.2, and colonization rates $c_i$ are evenly spaced between 0.45 and 0.8.

The time-averaged model does not capture stochastic extinctions of species at low abundances (demographic stochasticity). This means that no matter how low abundances fall after a disturbance event, they can always recover. This allowed us to

average over the disturbances without ignoring stochastic extinctions. While ignoring the effect of demographic stochasticity is a limitation of our model, this limitation becomes irrelevant if we assume there are rare species-reintroduction events from outside the system. Then, species which have been knocked extinct by a particularly violent disturbance event will be reintroduced, and get a chance to recover again. Putting it differently, the global dynamical stability of feasible $n$-species equilibria (Appendix S3) means that when we remove one of the species, this reduced system is unstable against the reintroduction of the removed species. Thus, assuming an ever so small rate of immigration from outside can counteract stochastic extinctions and keep our results intact even in the face of demographic stochasticity.

**Supporting Information.** Liao, J., G. Barabás, and D. Bearup. 2021. Competition-colonization dynamics and multimodality in diversity-disturbance relationships. Ecology.

## Appendix S3

### Section S1. Local and global stability of feasible equilibria

As shown in Appendix S2, the time-averaged model can be written as

$$\frac{d\bar{p}_i}{dt} = \bar{p}_i\left(\bar{b}_i + \sum_{j=1}^{n} A_{ij}\bar{p}_j\right), \qquad \text{Equation S1}$$

where $\bar{b}_i = c_i - e_i + \log(1-D)/T$ is the time-averaged effective intrinsic growth rate (colonization minus extinction, plus the time averaged disturbance effect), and $A_{ij} = c_i H_{ij} - c_j H_{ji} - c_i$ is the effective interaction matrix. Here we show that as long as the matrix $H$ is fully hierarchical ($H_{ij} = 1$ if $i < j$ and $0$ otherwise), any feasible equilibrium point is stable.

Since Appendix S3: Equation S1 is an effective Lotka–Volterra system, it has at most one fixed point, $\bar{p}_i^* = -\sum_{j=1}^{n} (A^{-1})_{ij}\bar{b}_j$, where all equilibria $\bar{p}_i^*$ are positive. Let us assume that this fixed point is indeed feasible. The Jacobian matrix $J$ of Appendix S3: Equation S1, evaluated at this equilibrium, has entries $J_{ik}^* = \bar{p}_i^* A_{ik}$. Indeed,

$$J_{ik} = \frac{\partial\left(d\bar{p}_i/dt\right)}{\partial \bar{p}_k} = \frac{\partial}{\partial \bar{p}_k}\left[\bar{p}_i\left(\bar{b}_i + \sum_{j=1}^{n} A_{ij}\bar{p}_j\right)\right]$$
$$= \delta_{ik}\left[\bar{b}_i + \sum_{j=1}^{n} A_{ij}\bar{p}_j\right] + \bar{p}_i A_{ik}, \qquad \text{Equation S2}$$

where $\delta_{ik} = 1$ if $i = k$ and $0$ otherwise. We evaluate this expression at $\bar{p}_i^*$ to get

$$J_{ik}^* = \delta_{ik}\underbrace{\left[\bar{b}_i + \sum_{j=1}^{n} A_{ij}\bar{p}_j^*\right]}_{0} + \bar{p}_i^* A_{ik} = \bar{p}_i^* A_{ik}. \qquad \text{Equation S3}$$

The braced term was by Appendix S3: Equation S1. At equilibrium, $d\overline{p}_i/dt$ is zero, so based on the right hand side of Appendix S3: Equation S1, either $\overline{p}_i^*$ or the term in parentheses (which is identical to the braced term above) is zero. Since the equilibrium is assumed to be feasible, $\overline{p}_i^* > 0$, and the braced term disappears.

With a fully hierarchical matrix $H$, $A_{ij}$ is lower triangular. This is because in the upper triangle ($i < j$), the nonzero contribution is $c_i H_{ij} - c_i$; but since $H_{ij} = 1$ for $i < j$, we have $c_i - c_i = 0$ for all $i < j$. In turn, the lower triangular part ($i > j$) is $A_{ij} = -c_j H_{ji} - c_i = -c_j - c_i$; and the diagonal entries are simply equal to $-c_i$. Thus the matrix $A$ has the following structure:

$$A = -\begin{pmatrix} c_1 & 0 & 0 & \cdots & 0 \\ c_1 + c_2 & c_2 & 0 & \cdots & 0 \\ c_1 + c_3 & c_2 + c_3 & c_3 & \cdots & 0 \\ \vdots & \vdots & \vdots & \ddots & \end{pmatrix}. \qquad \text{Equation S4}$$

This means that $J_{ij}^* = \overline{p}_i^* A_{ij}$ is also lower triangular, with the $i$th row of $A$ above is multiplied by $\overline{p}_i^*$:

$$J^* = -\begin{pmatrix} \overline{p}_1^* c_1 & 0 & 0 & \cdots & 0 \\ \overline{p}_2^* (c_1 + c_2) & \overline{p}_2^* c_2 & 0 & \cdots & 0 \\ \overline{p}_3^* (c_1 + c_3) & \overline{p}_3^* (c_2 + c_3) & \overline{p}_3^* c_3 & \cdots & 0 \\ \vdots & \vdots & \vdots & \ddots & \end{pmatrix}. \qquad \text{Equation S5}$$

The local stability of the equilibrium point is determined by the eigenvalues of this matrix. But a triangular matrix's eigenvalues $\lambda_i$ are simply the diagonal entries themselves. In this case, $\lambda_i = -\overline{p}_i c_i$, which are manifestly real and negative, indicating that any feasible $n$-species equilibrium point is stable.

In case $H$ is not fully hierarchical, the above argument no longer applies. However, since eigenvalues are continuous functions of the matrix entries (they are roots of the characteristic polynomial), a sufficiently small perturbation of the perfect

hierarchy will not be able to change the signs of the eigenvalues' real parts from negative to positive. Thus, the above stability result will still hold for sufficiently small departures from a perfect hierarchy.

When the matrix $H$ is fully hierarchical, the feasible, locally stable equilibrium point is also globally stable. This follows from the fact that a hierarchical $H$ leads to an effective interaction matrix $A$ whose upper triangular entries are all zero. Then Appendix S3: Equation S1 gives, for species $i = 1$

$$\frac{d\bar{p}_1}{dt} = \bar{p}_1(\bar{b}_1 + A_{11}\bar{p}_1). \qquad \text{Equation S6}$$

This is a simple logistic equation for $\bar{p}_1$, therefore it reaches its equilibrium value $\bar{p}_1^*$ from any positive initial condition. Turning to the second species:

$$\frac{d\bar{p}_2}{dt} = \bar{p}_2(\bar{b}_2 + A_{21}\bar{p}_1 + A_{22}\bar{p}_2). \qquad \text{Equation S7}$$

But since species 1 grows logistically, it will eventually reach its equilibrium $\bar{p}_1^*$. At that point, we have $\frac{d\bar{p}_2}{dt} = \bar{p}_2(\bar{b}_2 + A_{21}\bar{p}_1 + A_{22}\bar{p}_2)$, where $\bar{b}_2 + A_{21}\bar{p}_1^*$ is a constant. Then it can be thought of as an effective intrinsic growth rate, and the above equation is again just a logistic equation, with a globally stable equilibrium. And so on, for each subsequent species – due to $A$ having zeros in the upper triangle, the right hand side always depends only on species below $i$ in the hierarchy, and thus the overall long-term growth is logistic for each species. This proves that the feasible equilibrium is not just locally, but also globally stable.

**Supporting Information.** Liao, J., G. Barabás, and D. Bearup. 2021. Competition-colonization dynamics and multimodality in diversity-disturbance relationships. Ecology.

**Appendix S4**

**Section S1. The checkerboard pattern of the inverse community matrix**

Here we show that the observed relative abundance patterns in Fig. 2 of the main text can be understood from the equation

$$\bar{p}_i^* = -\sum_{j=1}^{n} (A^{-1})_{ij} [c_j - e_j + log(1-D)/T] \qquad \text{Equation S1}$$

(see Appendix S2: Equation S8), which yields giving the average long-term patch occupancies as a function of disturbance extent. The effective interaction matrix $A$ has entries $A_{ij} = c_i H_{ij} - c_j H_{ji} - c_i$ (Appendix S2: Equation S2). Here we assume that the matrix $H$ is fully hierarchical: $H_{ij} = 1$ if $i < j$ and 0 otherwise. As such, $c_i H_{ij} - c_i$ cancels each other for upper triangular ($i < j$) entries, and $A$ reduces to $-(c_j + c_i)$ in the lower triangular entries and to $-c_i$ along its diagonal. Introducing the matrices $C$ and $L$, where $C$ is diagonal with its $i$-th diagonal entry equal to $-c_i$, and $L$ is lower triangular with entries $L_{ij} = -(c_i + c_j)\Theta_{ij}$ (where $\Theta_{ij} = 1$ for $i > j$ and $0$ otherwise), we can then write $A$ as the sum of the two: $A = C + L$.

Since all $c_i > 0$, the diagonal matrix $C$ is invertible. Its inverse $C^{-1}$ is itself a diagonal matrix with the $-1/c_i$ along its diagonal. One can then equivalently write $A = C + L$ as

$$A = C(I + C^{-1}L). \qquad \text{Equation S2}$$

The inverse of $A$ as a whole can thus be written as

$$A^{-1} = (I + C^{-1}L)^{-1}C^{-1}.$$ Equation S3

We now use the known identity $(I - B)^{-1} = \sum_{k=0}^{\infty} B^k$ that holds for any matrix $B$ with eigenvalues falling inside the unit circle (the Neumann series expansion). In our case, $B = -C^{-1}L$, a strictly lower triangular matrix. The eigenvalues of strictly lower triangular matrices are all equal to $0$ (these matrices are nilpotent), which do of course fall in the unit circle. The Neumann series expansion therefore holds, and we can write

$$A^{-1} = \sum_{k=0}^{\infty}(-1)^k(C^{-1}L)^k C^{-1}.$$ Equation S4

Even more is true: since the $n$-th power of a strictly lower triangular matrix is guaranteed to vanish, we can terminate the above infinite sum at $n-1$:

$$A^{-1} = \sum_{k=0}^{n-1}(-1)^k(C^{-1}L)^k C^{-1}.$$ Equation S5

For the following, it will be easier if we multiply both sides by $C$ from the right, and work with $A^{-1}C$:

$$A^{-1}C = \sum_{k=0}^{n-1}(-1)^k(C^{-1}L)^k.$$ Equation S6

Let us examine the powers of $C^{-1}L$ in more detail. Its $0$-th power is simply the identity matrix: $(C^{-1}L)^0 = I$, or $(C^{-1}L)^0_{ij} = \delta_{ij}$ for its $(i,j)$-th entry (the Kronecker symbol $\delta_{ij}$ is $1$ if $i = j$ and $0$ otherwise). The $(i,j)$-th entry of the first power $(C^{-1}L)^1 = C^{-1}L$ reads, using $L_{ij} = -(c_i + c_j)\Theta_{ij}$, as

$$(C^{-1}L)_{ij} = \sum_{k=1}^{n}\frac{1}{c_i}\delta_{ik}(c_k + c_j)\Theta_{kj} = \left(1 + \frac{c_j}{c_i}\right)\Theta_{ij},$$ Equation S7

with $\Theta_{ij}$ restricting its nonzero entries below the main diagonal. The $(i,j)$-th entry of the second power is

$$(C^{-1}L)^2_{ij} = \sum_{k=1}^{n}\left(1 + \frac{c_k}{c_i}\right)\left(1 + \frac{c_j}{c_k}\right)\Theta_{ik}\Theta_{kj} = \sum_{k=j+1}^{i-1}\left(1 + \frac{c_k}{c_i}\right)\left(1 + \frac{c_j}{c_k}\right),$$ Equation S8

where the summation is understood to yield zero if $j+1>i-1$. Clearly, as long as $j+1\leq i-1$, the contribution of $(C^{-1}L)^2$ to the $(i,j)$-th entry always exceeds the contribution of $C^{-1}L$ (since the $c_i$ are all positive). The condition $j+1\leq i-1$ restricts the entries of $(C^{-1}L)^2$ below the first subdiagonal. A similar argument establishes that the nonzero entries of $(C^{-1}L)^3$ exceed the corresponding ones in $(C^{-1}L)^2$ (and are restricted to below the second subdiagonal), and so on: $(C^{-1}L)^k>(C^{-1}L)^{k-1}$ for entries below the $(k-1)$-th subdiagonal.

As seen from Appendix S4: Equation S6, $(C^{-1}L)^k$ is multiplied by $(-1)^k$ in the summation. When summing over $k$, the main diagonal is $(-1)^0(C^{-1}L)^0=I$. The first subdiagonal is given by the corresponding entries of $-C^{-1}L$, which are all negative. The second subdiagonal is determined by the corresponding entries of $-C^{-1}L+(C^{-1}L)^2$; however, since we established that the nonzero entries of $(C^{-1}L)^k$ exceed those of $(C^{-1}L)^{k-1}$, these entries will be positive. Continuing the same argument, the entries in the second subdiagonal $\left[-C^{-1}L+(C^{-1}L)^2-(C^{-1}L)^3\right]$ will again be negative; the ones in the 4-th subdiagonal positive, and so on: the subdiagonals keep alternating signs.

All this is true for $A^{-1}C$ (Appendix S4: Equation S6). To obtain $A^{-1}$ itself, to be used in Appendix S4: Equation S1, we multiply from the right with the diagonal matrix $C^{-1}$. Its effect is to multiply each column of $A^{-1}C$ by $-1/c_i$. This flips the sign of each entry and adjusts the magnitudes of the nonzero entries, without affecting the alternating sign-pattern in $A$, which therefore looks like this:

$$A^{-1} = \begin{pmatrix} - & 0 & 0 & 0 & \cdots & 0 \\ + & - & 0 & 0 & \cdots & 0 \\ - & + & - & 0 & \cdots & 0 \\ + & - & + & - & \cdots & 0 \\ \vdots & \vdots & \vdots & \vdots & \ddots & \end{pmatrix}. \qquad \text{Equation S9}$$

Let us now see what happens when the top species in the hierarchy (species 1) goes extinct. It is reasonable to expect this species to be the first to disappear as the disturbance extent $D$ increases, because the top species also has the lowest $c_i$. Thus, the increased mortality due to disturbance will bring the intrinsic growth of the top species below zero before other species, which guarantees its extinction. The effect of species 1 on the other species is summarized by the first column of $A$: species 2 is positively affected by species 1, species 3 negatively, species 4 positively again, and so on. Thus, the removal of species 1 hurts 2, helps 3, hurts 4 again etc., resulting in a sharp change in the trajectories of all $\bar{p}_i^*$ as a function of increasing $D$ (Appendix S4: Equation S1). If the effect is strong enough to not just change the trajectory but turn increasing ones into decreasing ones and vice versa, then the pattern in Fig. 2 of the main text is established. With a fully hierarchical matrix *H*, we thus prove that $A^{-1}$ is a lower triangular matrix whose non-zero entries alternate their signs (+ or –) in a checkerboard pattern. More specifically, when the topmost species in the hierarchy is removed, the direction of the trajectory of $\bar{p}_i^*$ suddenly changes.

In fact, while we did not manage to find a formal proof, even more is true: any entry $(A^{-1})_{ij}$ with $i > j$ is such that

$$\left|(A^{-1})_{ij}\right| \geq \sum_{k=j+1}^{i} (A^{-1})_{ik} \quad (i > j). \qquad \text{Equation S10}$$

The consequence is that the extinction of the current top species will indeed change increasing $\bar{p}_i^*(D)$ curves to decreasing ones, and vice versa. This conjecture held in

every case we checked, and we suspect it is in fact a theorem. However, even if one treats it as just a well-supported conjecture, it helps explain the pattern of Fig. 2 in the main text and therefore the ubiquity of the oscillating diversity-disturbance patterns.

Finally, these results are maintained even if the matrix $H$ is not fully hierarchical. By the general continuity of the $A \mapsto A^{-1}$ mapping that holds for any invertible matrix, a sufficiently small change in $H$ can only cause a small change in $A^{-1}$. If $H$ is still upper triangular, then a small enough change cannot alter the sign pattern of Appendix S4: Equation S9. If $H$ is no longer upper triangular, then the upper triangular entries of $A^{-1}$ will no longer be exactly zero – however, as long as the deviation of $H$ from upper triangularity is small, this will not override the overall $\overline{p_i}^*(D)$ patterns as shown in Fig. 2.

**Supporting Information.** Liao, J., G. Barabás, and D. Bearup. 2021. Competition-colonization dynamics and multimodality in diversity-disturbance relationships. Ecology.

**Appendix S5 - *Figures S1-S7***

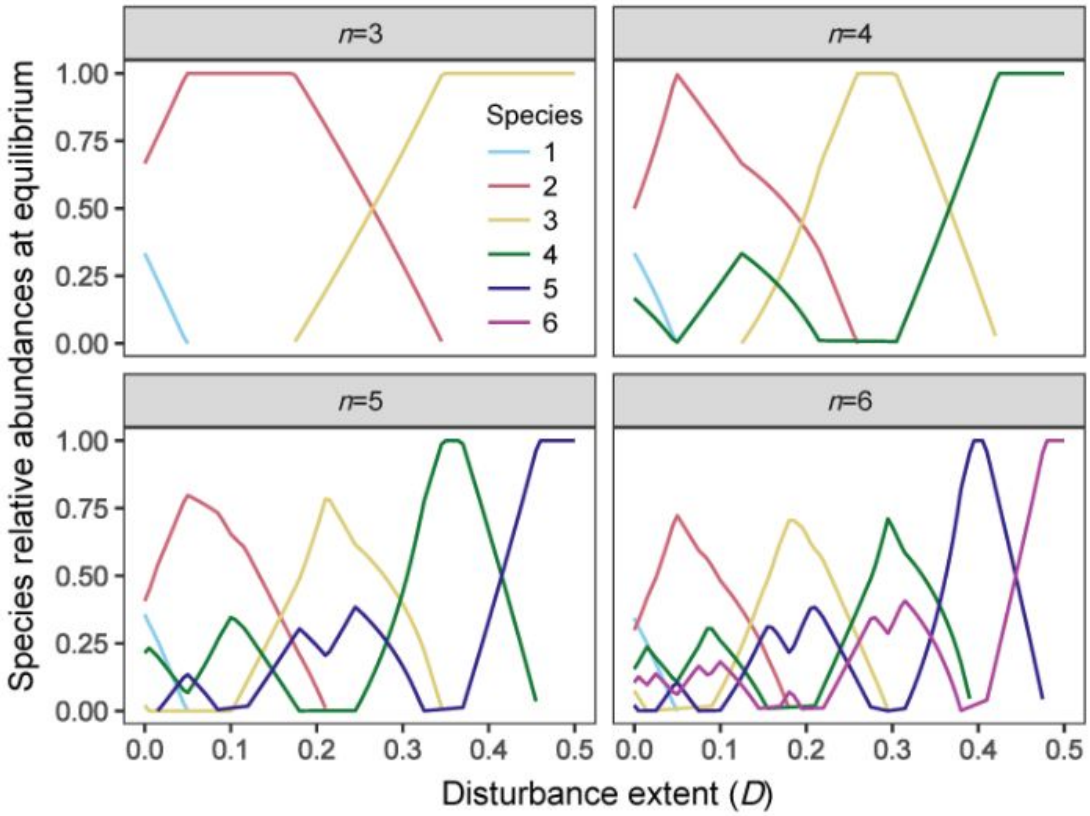


**Figure S1. Effect of disturbance extent on species relative abundances in multispecies systems** ($n$=3, 4, 5, 6; species denoted by color lines) with a high spread of vital rates (evenly spaced $c_i \in [0.25, 1]$), simultaneously considering a strict competitive hierarchy. Other parameter values are the same as in Fig. 1.

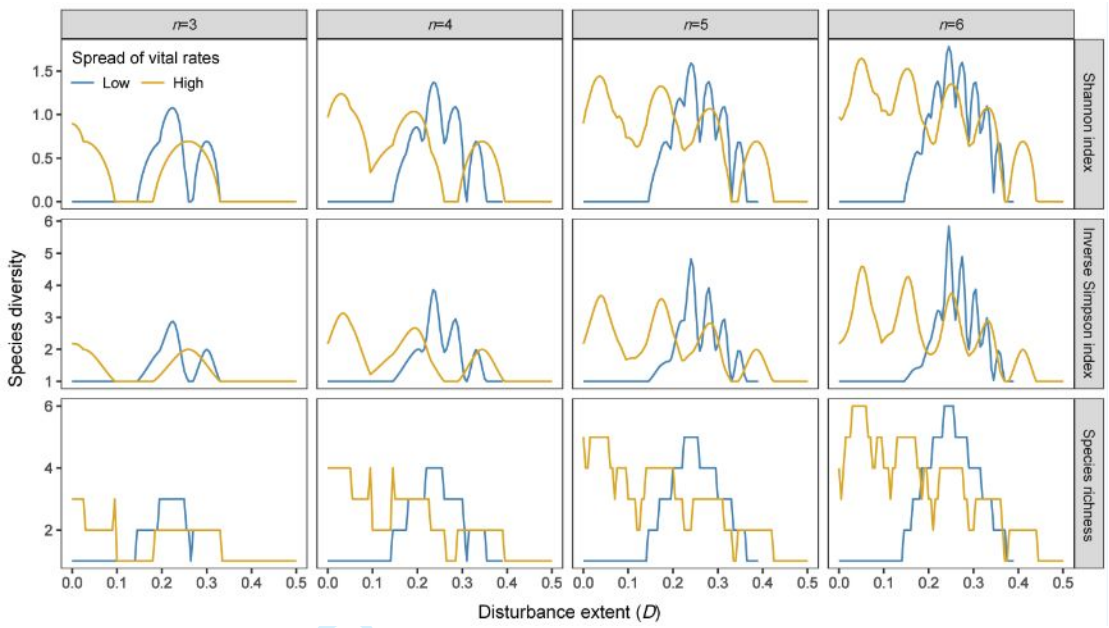


**Figure S2. Diversity-disturbance curves in multispecies systems** ($n$=3, 4, 5, 6) with a strict competitive hierarchy, simultaneously by considering both low (blue lines: evenly spaced $c_i \in [0.5, 0.7]$) and high (yellow lines: evenly spaced $c_i \in [0.3, 0.9]$) spreads by fixing the mean $\bar{c}$=0.6. Other parameters are the same as in Fig. 1.

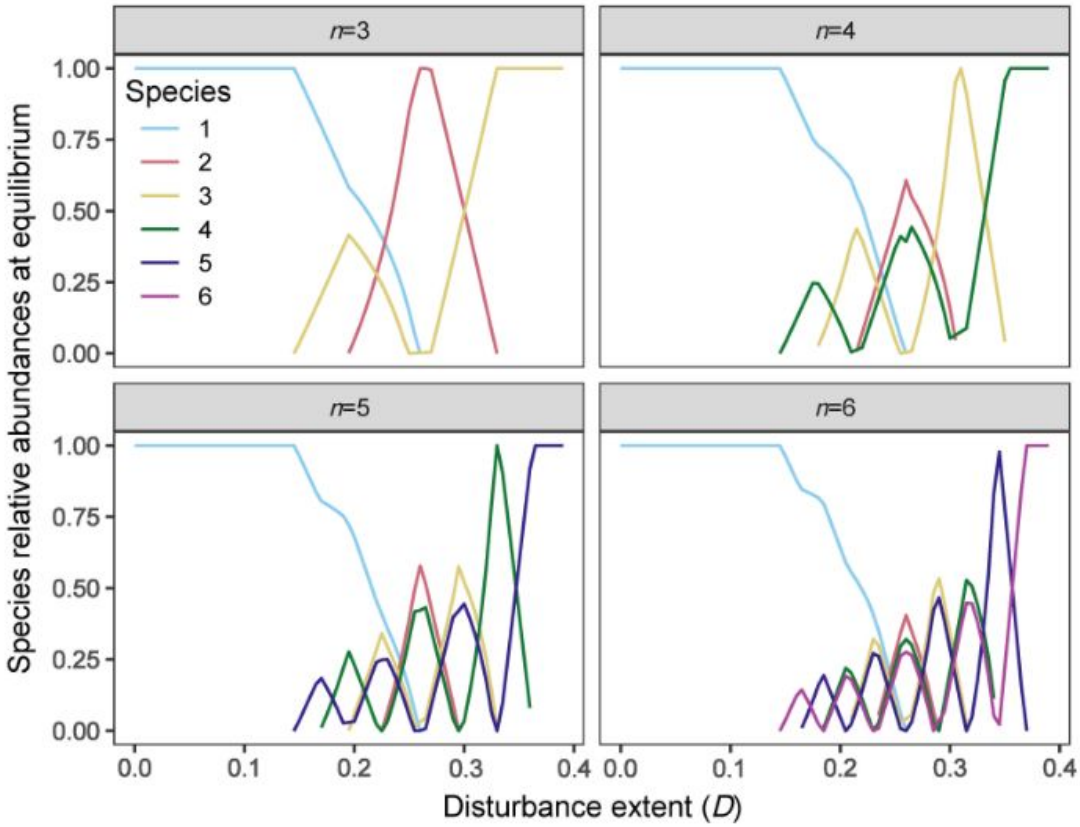


**Figure S3. Effect of disturbance extent on species relative abundances in multispecies systems** ($n$=3, 4, 5, 6; species denoted by color lines) with a low spread of vital rates (evenly spaced $c_i \in [0.5, 0.7]$), simultaneously considering a strict competitive hierarchy. Other parameters seen in Appendix S5: Fig. S2.

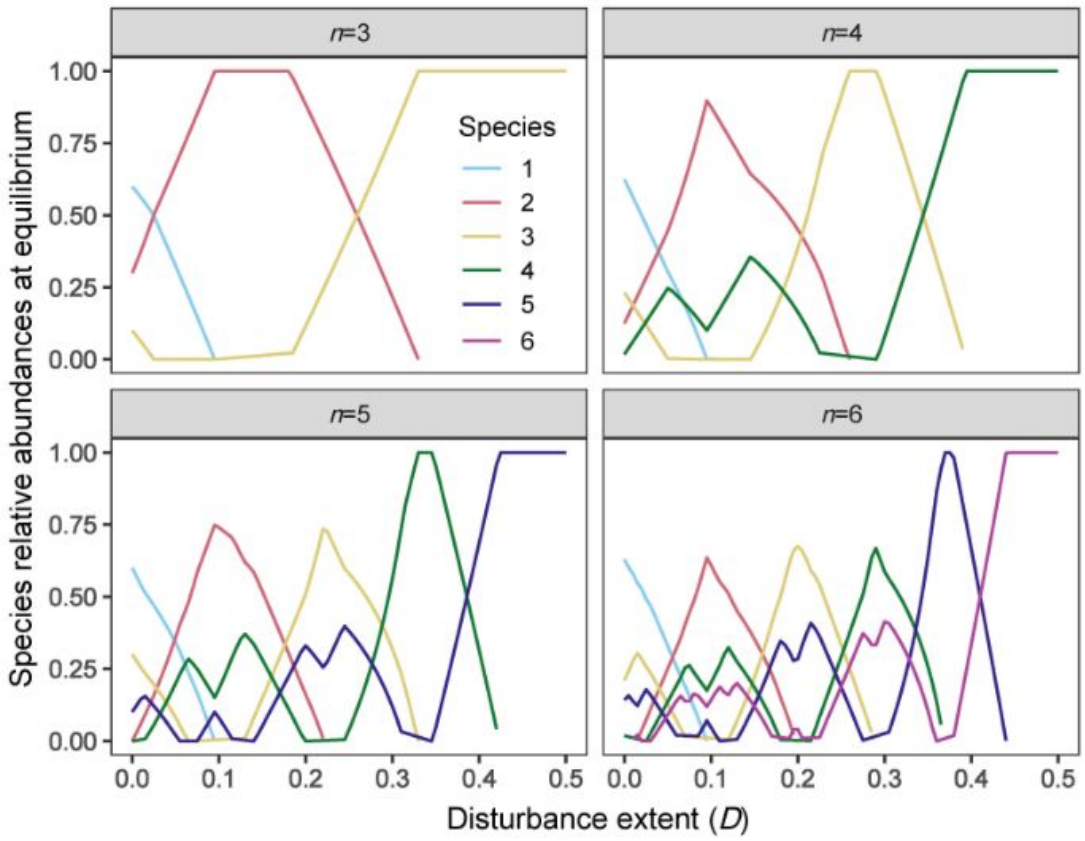


**Figure S4. Effect of disturbance extent on species relative abundances in multispecies systems** ($n$=3, 4, 5, 6; species denoted by color lines) with a high spread of vital rates (evenly spaced $c_i \in [0.3, 0.9]$), simultaneously considering a strict competitive hierarchy. Other parameters seen in Appendix S5: Fig. S2.

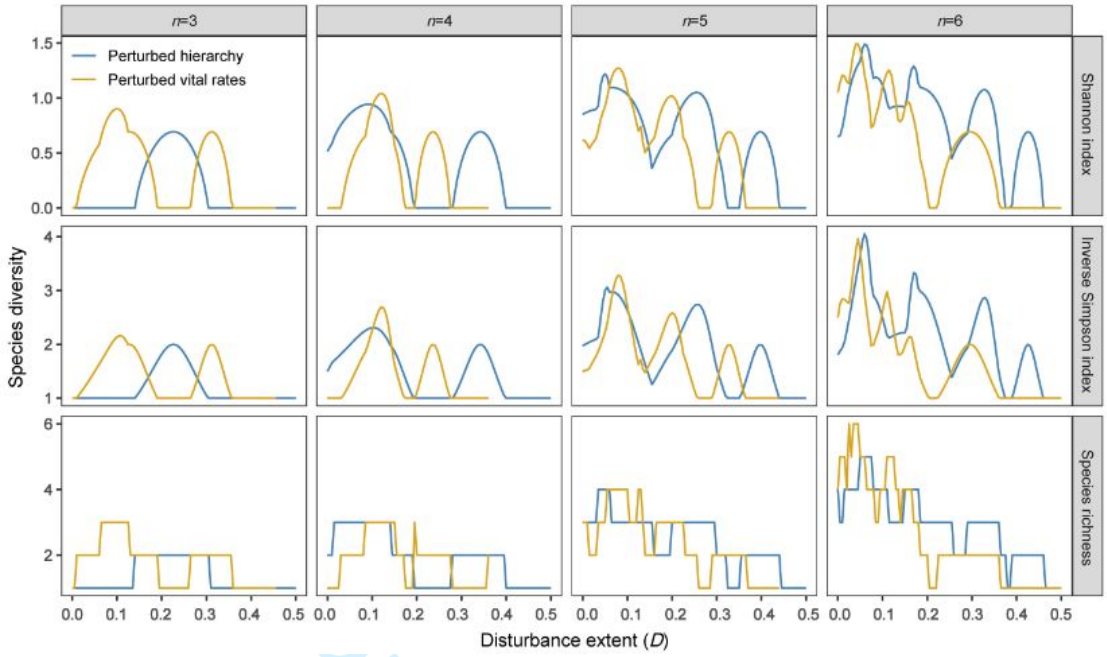


**Figure S5. Diversity-disturbance curves in multispecies systems** ($n$=3, 4, 5, 6), by considering two cases. First, species colonization rates are evenly spaced from $c_i \in [0.25,1]$ while perturbing the competitive hierarchy $H$: the upper triangular entries are uniformly sampled from $H_{ij} \in [0.75, 1]$ while the lower triangular ones from $H_{ij} \in [0, 0.25]$ (blue lines). Second, species colonization rates are uniformly drawn from $c_i \in [0.25, 1]$ and sorted in increasing order, but with a strict competitive hierarchy $H$ (yellow lines). Other parameters: see Fig. 1.

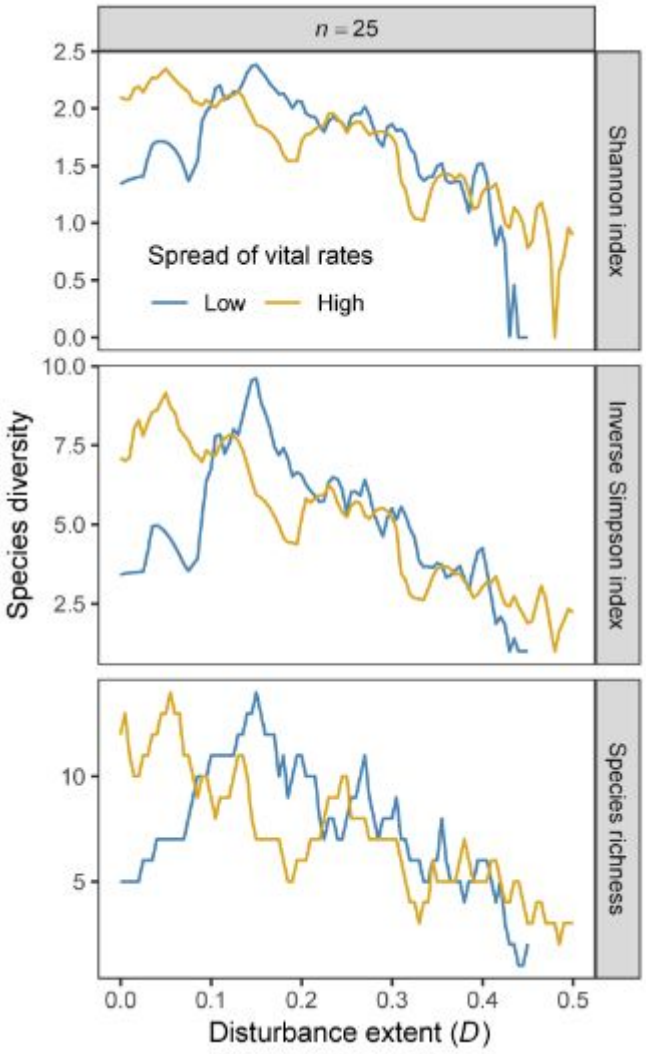


**Figure S6. Diversity-disturbance curves in a highly diverse community** ($n$=25), with a large perturbation to the competitive hierarchy $H$: the upper triangular entries are uniformly sampled from $H_{ij}$∈[0.5, 1] while the lower triangular ones from $H_{ij}$∈[0, 0.5]. Species colonization rates are uniformly drawn from both low (blue lines: $c_i$∈[0.45, 0.8]) and high (yellow lines: $c_i$∈[0.25, 1]) spreads, and sorted in increasing order. Other parameters: Fig. 1.

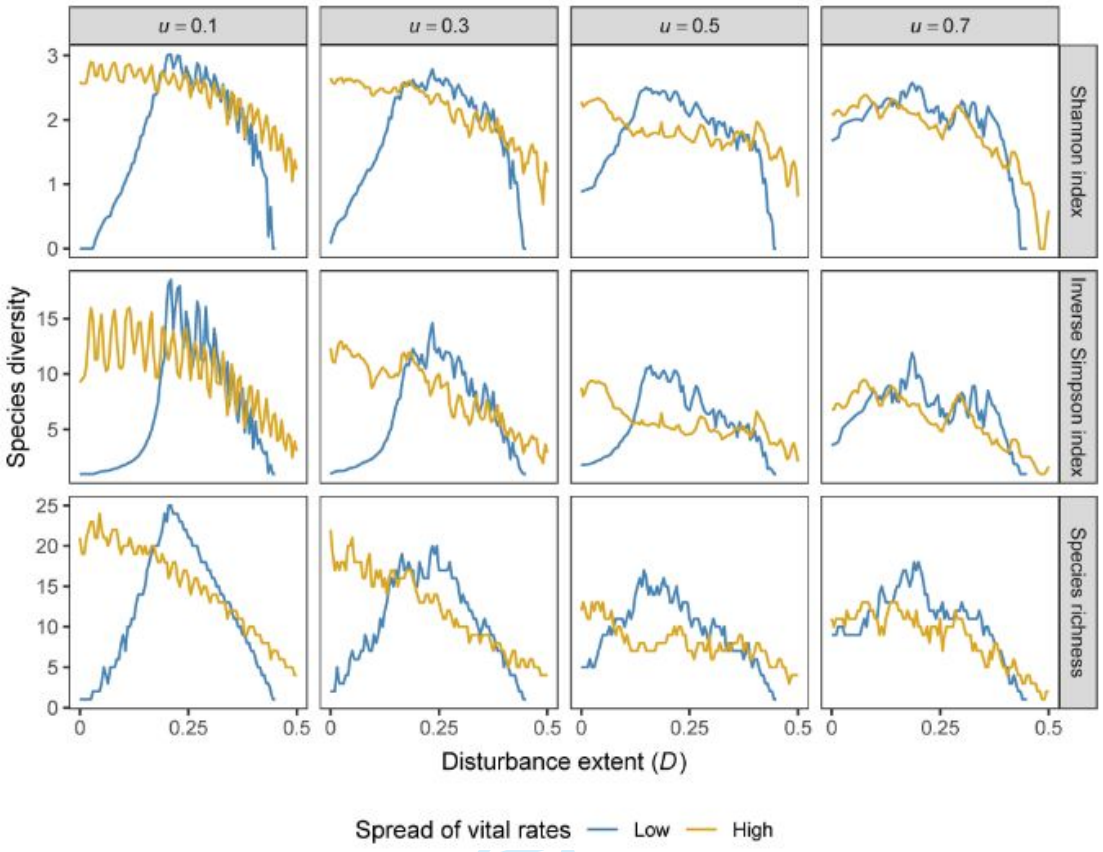


**Figure S7. Diversity-disturbance curves in a highly diverse community** ($n$=25), with different levels of violation ($u$=0.1, 0.3, 0.5 and 0.7) to the competitive hierarchy $H$: the upper triangular entries are uniformly sampled from $H_{ij} \in [1-u, 1]$ while the lower triangular ones from $H_{ij} \in [0, u]$. Species colonization rates are evenly spaced in both low (blue lines: $c_i \in [0.45, 0.8]$) and high (yellow lines: $c_i \in [0.25, 1]$) spreads. Other parameters: Fig. 1.

**Liao, J., G. Barabás, and D. Bearup. 2021. Competition-colonization dynamics and multimodality in diversity-disturbance relationships. Ecology.**

## Data S1

R code for diversity-disturbance relationships complied in DataS1.zip

## Authors

Jinbao Liao
Research Center for Theoretical Ecology, Jiangxi Normal University
Ziyang Road 99, 330022 Nanchang, China
Email: jinbaoliao@163.com

György Barabás
Division of Theoretical Biology, Department IFM, Linköping University
SE-58183 Linköping, Sweden
Email: dysordys@gmail.com

Daniel Bearup
University of Kent, School of Mathematics, Statistics and Actuarial Sciences
Parkwood Road, Canterbury, CT2 7FS, UK
Email: D.Bearup@kent.ac.uk

## File list (files found within DataS1.zip)

Diversity_disturbance.R

## Description

Diversity_disturbance.R – R code for diversity-disturbance relationships, including all simulation cases in the main text.